

See discussions, stats, and author profiles for this publication at: <https://www.researchgate.net/publication/5451217>

Entropic Changes Control the Charge Separation Process in Triads Mimicking Photosynthetic Charge Separation

ARTICLE *in* THE JOURNAL OF PHYSICAL CHEMISTRY A · JUNE 2008

Impact Factor: 2.69 · DOI: 10.1021/jp712008b · Source: PubMed

CITATIONS

26

READS

44

10 AUTHORS, INCLUDING:



Rodrigo E Palacios

Universidad Nacional de Río Cuarto

37 PUBLICATIONS 701 CITATIONS

SEE PROFILE



Gary F Moore

Arizona State University

46 PUBLICATIONS 694 CITATIONS

SEE PROFILE



Gerdenis Kodis

Arizona State University

75 PUBLICATIONS 2,397 CITATIONS

SEE PROFILE



Silvia Braslavsky

Max Planck Institute for Chemical Energy Co...

191 PUBLICATIONS 5,196 CITATIONS

SEE PROFILE

Entropic Changes Control the Charge Separation Process in Triads Mimicking Photosynthetic Charge Separation

Alberto C. Rizzi,^{†,‡} Maurice van Gastel,[†] Paul A. Liddell,[§] Rodrigo E. Palacios,[§] Gary F. Moore,[§] Gerdenis Kodis,[§] Ana L. Moore,[§] Tom A. Moore,[§] Devens Gust,[§] and Silvia E. Braslavsky^{*,†}

Max-Planck-Institut für Bioanorganische Chemie (formerly Strahlenchemie), Postfach 10 13 65, D-45413 Mülheim an der Ruhr, Germany, and Department of Chemistry and Biochemistry, Arizona State University, Tempe, Arizona 85287-1604

Received: December 21, 2007; In Final Form: February 8, 2008

Laser-induced optoacoustic spectroscopy (LIOAS) measurements with carotene–porphyrin–acceptor “supermolecular” triads (C–P–A, with A = C₆₀, a naphthoquinone NQ, and a naphthoquinone derivative, Q) were carried out with the purpose of analyzing the thermodynamic parameters for the formation and decay of the respective long-lived charge separated state C^{•+}–P–A^{•–}. The novel procedure of inclusion of the benzonitrile solutions of the triads in Triton X-100 micelle nanoreactors suspended in water permitted the separation of the enthalpic and structural volume change contributions to the LIOAS signals, by performing the measurements in the range 4–20 °C. Contractions of 4.2, 5.7, and 4.2 mL mol^{–1} are concomitant with the formation of C^{•+}–P–A^{•–} for A = C₆₀, Q and NQ, respectively. These contractions are mostly attributed to solvent movements and possible conformational changes upon photoinduced electron transfer, due to the attraction of the oppositely charged ends, as a consequence of the giant dipole moment developed in these compounds upon charge separation (~110 D). The estimations combining the calculated free energies and the LIOAS-derived enthalpy changes indicate that entropy changes, attributed to solvent movements, control the process of electron transfer for the three triads, especially for C–P–C₆₀ and C–P–Q. The heat released during the decay of 1 mol of charge separated state (CS) is much smaller than the respective enthalpy content obtained from the LIOAS measurements for the CS formation. This is attributed to the production of long-lived energy storing species upon CS decay.

Introduction

In the past decade several donor–bridge–acceptor “supermolecules” have been synthesized aiming at understanding and controlling the factors influencing photosynthetic energy and electron transfer (ET), with the ultimate goal of mimicking photosynthesis and the possible exploitation of photonic molecular devices. In particular, the construction of triads (C–P–C₆₀) including a carotene moiety (C) as electron donor and a fullerene (C₆₀) as electron acceptor has afforded the photoproduction of a charge separated state (CS) upon excitation of the porphyrin moiety (P), with a reported dipole moment of 153 ± 6 D.¹ Excitation of a carotene–porphyrin–naphthoquinone triad (C–P–Q) in a liposomal bilayer has demonstrated the vectorial photoinduced ET, because the generated C^{•+}–P–Q^{•–} eventually led to the pumping of protons across the membrane, driving in turn the ATP synthesis with the help of the enzyme ATP-synthase.²

The inclusion of C₆₀ in the “supermolecules” resulted in an acceleration of the intramolecular ET process and slowed down the charge recombination. Thus, a larger quantum yield of

charge separation and a longer-lived CS state are obtained with “supermolecules” containing a C₆₀ unit as a final electron acceptor.³ These effects have been attributed to the smaller reorganization energy of fullerenes as compared to planar acceptors, such as quinones and imides.⁴ The reorganization energy (λ), introduced by Marcus^{5,6} in the theory of ET and considered to be the sum of two factors: a solvent term, λ_s , and a vibrational term, λ_v , is one of the key factors determining the rate of an ET reaction.⁷

The technique of LIOAS has permitted to evaluate time-resolved structural volume changes, as well as enthalpy changes, in several types of photoinduced reactions.^{8–13} The structural volume change (ΔV_{str}), as derived from LIOAS measurements for a particular step in a photoinduced transformation, is also a sum of a solvent term and an intrinsic term.

When analyzing by LIOAS photoinduced intra- and intermolecular ET reactions of ruthenium complexes in aqueous solutions, we were able to identify the molecular origin of the ΔV_{str} values upon formation and decay of the metal-to-ligand excited states, as arising mostly from the photoinduced changes in strong specific chromophore–solvent interactions.^{14,15}

We decided then to analyze whether in “supermolecules” the ΔV_{str} values differ for different acceptors. For this purpose we studied by LIOAS the intramolecular ET reaction in three “supermolecules” consisting of carotene–porphyrin–acceptor (C–P–A) units with the same carotene, a very similar porphyrin, but different acceptors A, *i.e.*, C–P–C₆₀, C–P–Q, and

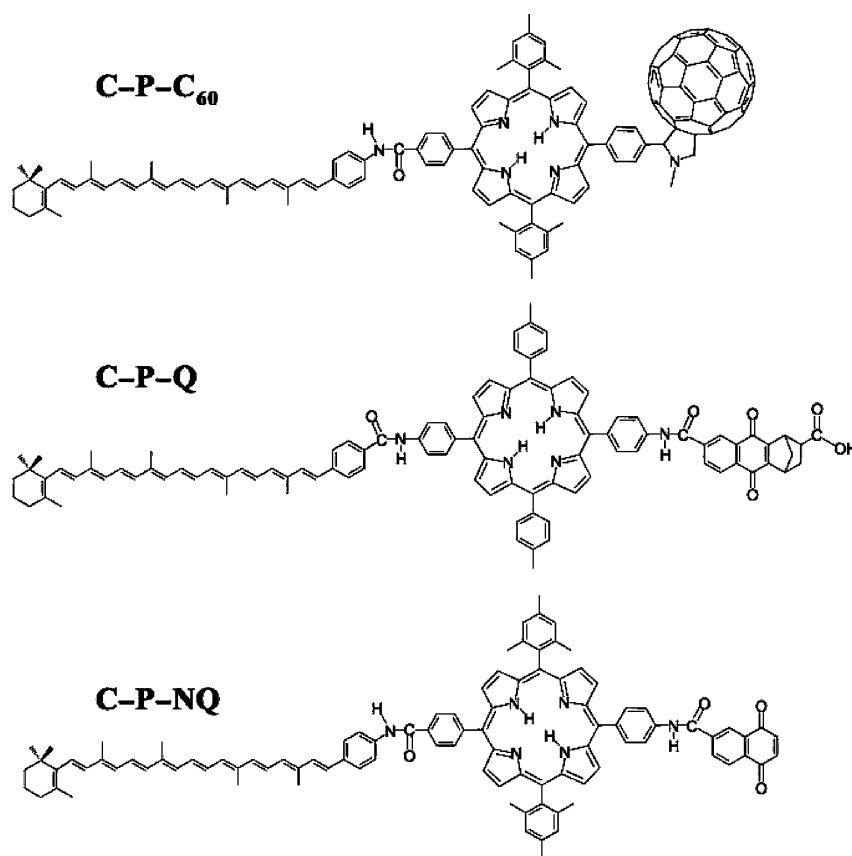
* Corresponding author. E-mail: braslavskys@mpi-muelheim.mpg.de. Fax: +49-208-306-3951.

[†] Max-Planck-Institut für Bioanorganische Chemie (formerly Strahlenchemie).

[‡] Present address: Departamento de Física, Facultad de Bioquímica y Ciencias Biológicas, Universidad Nacional del Litoral, Ciudad Universitaria, C.C. 242, 3000 Santa Fe, Argentina.

[§] Arizona State University.

SCHEME 1: Structural Formulas of the Three Compounds Employed



C-P-NQ with C₆₀, a naphthoquinone derivative, and naphthoquinone, respectively (Scheme 1). The three acceptors have relatively similar reduction potentials. In every case, upon laser-pulse excitation of the porphyrin, a rapid ET occurs to the acceptor A. Subsequently, the carotene donates an electron to the porphyrin to yield the $C^{+}-P-A^{\bullet-}$ species with a relatively long lifetime of tens or hundreds of nanoseconds.¹⁶

Depending on the conditions such as the structure of the carotenoid-porphyrin linkage, the solvent, and the temperature, this CS species recombines to yield the triad with the carotene in its triplet state, ${}^3C-P-A$. This has been thoroughly studied with C-P-C₆₀ dissolved in 2Me-THF, in which the decay of $C^{+}-P-C_{60}^{\bullet-}$ can yield the triplet ${}^3C-P-C_{60}$, which in turn decays to the ground state.^{16,17} The effects of the type of C-P linkage, temperature, and solvent, on the yield and output of the various photoinduced steps have been analyzed by Kuciauskas *et al.*³

One of the questions posed when analyzing these systems is what are the thermodynamic factors driving the various reaction steps. In particular, what is the relative role of the enthalpic and entropic factors (such as solvent reorganization).

Upon absorption of light, an excited molecular species decays by vibrational coupling with the solvent and by possible structural changes. These two phenomena contribute to the radiationless deactivation and can be measured as a pressure wave after laser-pulse excitation. The thermal contribution due to radiationless decay of the excited molecules produces a heat burst leading to a pressure wave. Possible structural volume changes (such as changes in bond strengths and angles and changes in the solvent-chromophore interactions due to changes in the chromophore dipole moment upon photoexcitation) also produce a volume change (the structural volume change, $\Delta_{\text{str}}V$)

that contributes to the pressure wave.^{11,13} The sum of both contributions gives rise to the acoustic signal. Because the thermal term directly depends on the thermal expansion coefficient [$\beta = 1/V(\partial V/\partial T)$], whereas the structural term does not, the two contributions are readily separated in aqueous solutions by changing the temperature of the measurements in a relatively small range (*e.g.*, 4–20 °C). For polar non-water soluble compounds, however, no procedure was available until recently for the separation of the two contributions to the LIOAS signal.⁹ We have already presented the method of inclusion of the water-immiscible organic solvent solutions of the “supermolecules” in water suspensions of detergent micelles, to separate both contributions to the LIOAS signal by changing the bulk temperature and taking into account that the thermoelastic properties of the bulk are mostly determined by its water content.¹⁸

We thoroughly develop in this paper this novel approach. The ET reaction is photoinduced in the polar molecules (the “supermolecules” in this case) dissolved in the polar water-immiscible solvent (such as benzonitrile) inside detergent micelles. These micelles act as nanoreactors, which isolate the “supermolecules” from the external environment. The variation of temperature induces changes in the value of β in the bulk aqueous medium without affecting the immediate environment of the reacting molecule.

Our results indicate that the formation of the CS state $C^{+}-P-A^{\bullet-}$ in the three super-molecules is determined by entropic factors that mainly arise from the solvent reorganization produced upon ET. Similar structural volume changes were found for CPNQ and CPC₆₀, whereas CPQ shows a larger $\Delta_{\text{str}}V$ for the formation of the CS state.

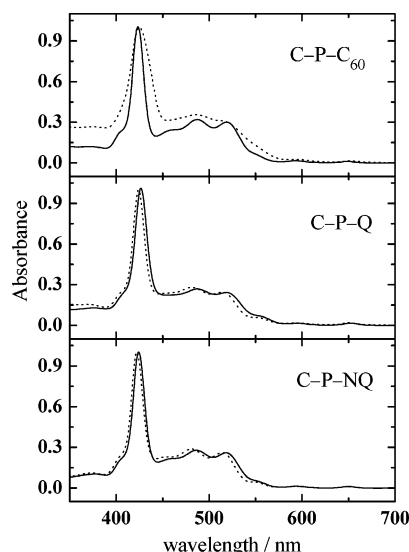


Figure 1. Absorption spectra (—) in neat BZN and (···) in BZN inside Triton X-100 aqueous micelles of C-P-C₆₀, C-P-Q, and C-P-NQ.

Experimental Section

Materials. The triads, *i.e.*, carotene–porphyrin–fullerene (C-P-C₆₀), carotene–porphyrin–naphthoquinone derivative (C-P-Q), and carotene–porphyrin–naphthoquinone (C-P-NQ) were synthesized as described by Kodis *et al.*,¹⁹ Hung²⁰ and Steinberg-Yfrach *et al.*,^{21,22} respectively. The calorimetric references azulene (Aldrich, 99%) and bromocresol green (BCG, Sigma, ACS reagent) were used as received. Triton X-100 (Sigma) and dodecyl-trimethylammoniumbromide (DTAB, Sigma, 99%) were used without further purification. Benzonitrile (BZN, Aldrich, 99.9% HPLC grade) and 2-methyltetrahydrofuran (2-Me-THF) (Aldrich, >99%) were used as received. Water was deionized and purified by a Millipore-Milli-Q System. Miscibility of BZN in water (and *vice versa*) was checked by gas chromatography. The solubility of BZN in H₂O was *ca.* 0.3% and that of H₂O in BZN was *ca.* 1.3%. This assured that the “supermolecules” were effectively dissolved in the organic phase of the micelles (*vide infra*).

A 0.1 M solution of Triton X-100 was prepared in water (critical micellar concentration of Triton X-100 *ca.* 10^{−3} M).²³ A 20 μ L aliquot of a BZN stock solution of suitable concentration of each of the triads or of the reference compound was injected into 3 mL of the detergent solution. After stirring, the initially turbid binary mixture transforms into a clear and optically isotropic solution. Addition of larger quantities of BZN stock solution produces irreversible turbid solutions.

Methods

UV–Vis Spectroscopy. UV–vis spectra of Triton X-100 micellar solutions of the reference azulene and of the three “supermolecules” (dissolved first in BZN and then incorporated into the Triton X-100 micelles) were recorded using a Shimadzu UV-2102 PC spectrophotometer. The spectra were similar to those in neat BZN (Figure 1), assuring that no changes in the absorption spectra are occurring during the dissolution of the compounds in the micro-heterogeneous media. However, the spectrum of C-P-C₆₀ is significantly broadened in the micelles; possible causes are triad aggregation or partitioning between the detergent layer and the BZN. In fact, in other detergents such as DTAB (instead of Triton X-100), the absorption spectrum of C-P-Q looked similar to the one in neat BZN

but for C-P-C₆₀ and C-P-NQ some absorption bands corresponding to the carotene seemed to disappear. We decided then to work with Triton X-100 which induced the smallest change in the absorption spectra of the triads.

LIOAS Experiments. The LIOAS setup has been already described in several papers.²⁴ For excitation, 11 ns laser pulses at 650 nm (the lowest energy porphyrin band) from a Nd:YAG laser (SL802, Spectron Laser Systems) pumped dye laser (SL4000G, Spectron Laser Systems, Rugby, U.K.) were employed, using DCM as the dye. The absorbance at the excitation wavelength for the calorimetric reference azulene and the samples in Triton X-100 micelle media was *ca.* 0.03 (the precise value depended on the particular sample). The beam was shaped by a 1 mm slit, which determines an acoustic transit time in aqueous solution of about 650 ns, allowing a time resolution of *ca.* 60 ns by deconvolution techniques.¹⁰ Incident laser energies were varied with a neutral density filter and the energies absorbed by the reference and the sample were measured with a pyroelectric energy meter (RJP735 head connected to a Rm-6600A Universal Radiometer, Laser Probe Inc.) and matched within 5% for reference and sample. This assured that sample and reference were measured under identical conditions at the wavelength of excitation, same bandwidth and also same temperature. The measurements were performed in the linear regime of amplitude *vs* laser radiant energy, which was up to 250 μ J/pulse. The total incident energy was *ca.* 150 μ J/pulse (fluence *ca.* 150 J m^{−2}). The acoustic wave was detected by a Pb–Zr–Ti ceramic piezoelectric transducer (PZT) (4 mm; Vernitron), amplified 100 times (Comlinear E103), digitized by a digital oscilloscope (Tektronik TDS 744A, operating at 500 megasample/s), and stored in a Compaq Tru64 Unix workstation and a personal computer for further treatment of the data. In total, 100 signals were averaged for each waveform. The cuvette holder FLASH 100 (Quantum Northwest, Spokane, WA) was temperature controlled to ± 0.02 °C. All triad solutions were degassed for 20 min with Ar before LIOAS measurements.

LIOAS Signal Handling. The procedure used to analyze the LIOAS signal has been widely described in many publications and has also been reviewed.¹⁰ Deconvolution techniques are required to analyze the time evolution of the pressure when transient species are produced with lifetimes within the acoustic transient time. The signal of the sample is regarded as a convolution of the instrumental response obtained with a calorimetric reference and a sum of single-exponential terms that describe the time evolution of the pressure in the sample after laser excitation. The analysis yielded the fractional amplitudes (φ_i) and the lifetimes (τ_i) of the transients occurring during the *i*th step of the photoinduced reaction. The analysis was performed by the package Sound Analysis v. 1.50D, 1999, Quantum Northwest Inc., Spokane, WA. With a 1 mm slit (*vide supra*) lifetimes between 60 ns and a few microseconds can be resolved with this approach. The fractional amplitudes (φ_i) contain information about the heat released (q_i) and the structural volume change ($\Delta_{\text{str},i}V$) for each process *i* and is expressed by

$$\varphi_i = \frac{q_i}{E_\lambda} + \Phi_i \frac{\Delta_{\text{str},i}V}{E_\lambda} \left(\frac{c_p r}{\beta} \right)_T \quad (1)$$

with E_λ the molar excitation energy (650 nm \equiv 183.98 kJ mol^{−1}), Φ_i the quantum yield of the *i*th step, c_p the specific heat capacity at constant pressure, ρ the density of the solution, and $\beta = (\partial V / \partial T)_p / V$ the volume expansion coefficient. Because β strongly depends on the temperature in aqueous solutions (a unique property of water and aqueous solutions whereas this

parameter varies negligibly with temperature for organic solvents), the separation of q and $\Delta_{\text{str}}V$ was made possible by using aqueous suspensions of micelles enclosing the triads dissolved in BZN and by measuring in a relatively narrow temperature range (4–20 °C).¹³

The ratio of thermoelastic parameters $(c_p\rho/\beta)_{\text{Tx}}$ (Tx = Triton X-100) of the micellar media was determined by comparison with the ratio for neat BZN $[(c_p\rho/b)_{\text{BZN}}$, taken from tables] following a methodology similar to that previously described for inverted micelles.²⁵ For this purpose, the amplitude of the LIOAS signals of the calorimetric reference azulene dissolved in BZN, H^{BZN} , was compared to that of the same reference dissolved in BZN and incorporated into the Triton X-100 micelles, H^{Tx} . The isothermal compressibilities, κ_T , of both BZN and Triton X-100 micelle media are needed to calculate the ratio of thermoelastic parameters $(c_p\rho/\beta)_{\text{Tx}}$ in the microheterogeneous Triton X-100/BZN/water micelle medium (eq 2).¹⁰

$$\frac{\left(\frac{c_p\rho}{\beta}\right)_{\text{Tx}}}{\left(\frac{c_p\rho}{\beta}\right)_{\text{BZN}}} = \frac{\kappa_T^{\text{BZN}}}{\kappa_T^{\text{Tx}}} \frac{H_R^{\text{BZN}}}{H_R^{\text{Tx}}} \quad (2)$$

The isothermal compressibility κ_T is expressed as the sum (eq 3) of the adiabatic compressibility κ_S plus a term $(T\beta^2/c_p\rho)$

$$\kappa_T = \kappa_S + T \frac{\beta^2}{c_p\rho} \quad (3)$$

calculated with values from tables for BZN or approximated for the case of the micelle-solutions taking into account the molar fraction of the micelles and the thermoelastic parameters of water.²⁵ The value of $\kappa_S = 1/(\rho v_a^2)$ is calculated with eq 3 knowing the velocity of sound v_a and the density ρ of the micelle media at each temperature.¹⁰

The sound velocity v_a in the aqueous media and in BZN was measured by comparing the times required by the acoustic wave to arrive to the piezoelectric detector. These times were measured with the calorimetric reference BCG in water (azulene is not soluble in water) and in neat BZN, and with the calorimetric reference azulene in the Triton X-100/BZN aqueous micelle medium and in neat BZN, all at the same temperature at which the LIOAS signals of the triads solutions were measured. The velocity of sound in neat BZN determined by this method ($1.42 \times 10^3 \text{ m s}^{-1}$) is in good agreement with the value reported in the literature.²⁶ The density of the solutions was measured by pycnometry.

Transient Absorbance Experiments. The nanosecond transient absorption decays were measured in Triton X-100/BZN aqueous micelle solutions for the three triads upon excitation with pulses from an Oportek OPO (optical parametric oscillator) pumped by the third harmonic of a Continuum Surelight Nd:YAG laser. The pulse width was *ca.* 5 ns and 10 nm bandwidth, and the repetition rate was 5 Hz. The part of the spectrometer used for detection has been described elsewhere.²⁷ All solutions were degassed for 20 min with Ar prior to the measurements. C–P–C₆₀ dissolved in 2Me-THF ($\Phi_{\text{CS}} = 1$) was used as the reference for the calculation of quantum yields.¹⁹ Indices of refraction of the solutions were measured with an Atago Abbe 3T NAR-3T refractometer.

Time-Resolved Electron Paramagnetic Resonance (TR-EPR). TR-EPR experiments were performed at $T = 40 \text{ K}$ on a Bruker ESP380E spectrometer equipped with an ER 4118 SPT cylindrical cavity and a continuous flow helium cryostat (Oxford

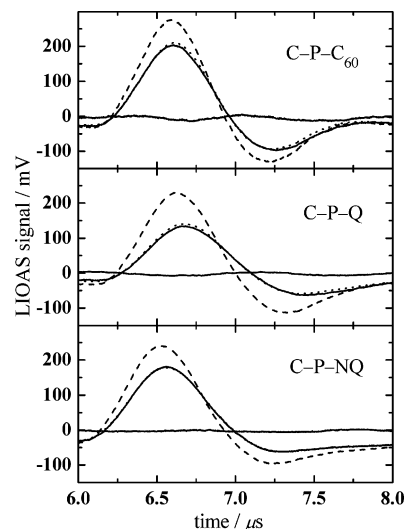


Figure 2. Energy-normalized LIOAS signals upon 650 nm excitation of the reference azulene (dashed lines) and C–P–C₆₀, C–P–Q, and C–P–NQ (full lines), each dissolved in BZN and encapsulated in Triton X-100 aqueous micelles and all at 10 °C. The simulation of the signal (dotted lines overlapping the sample signals), when using a sequential three-single-exponential function, and the residual distribution around zero are also shown in each case. The absorbances of the triads and reference micelle solutions A(650 nm) were *ca.* 0.03 (the precise value depended on the sample).

Instruments). Laser excitation at 650 nm was provided by a Nd:YAG laser (Spectra Physics, GCR-130) and an OPO system (GWU-Lasertechnik, Erfstadt, Germany). The pulse width was 6–7 ns, the repetition frequency was 10 Hz and the energy per pulse from the laser was *ca.* 9 mJ/pulse. The microwave frequency was 9.77 GHz and the microwave power 2 mW. No field modulation was used. The transient signal was recorded with a Lecroy 9450A oscilloscope. All solutions were degassed 20 min with Ar prior to the measurements.

Fluorescence. Steady state fluorescence spectra were measured using a Varian Cary Eclipse Fluorolog spectrofluorometer. Cresyl violet in methanol was used as a standard (fluorescence quantum yield, $\Phi_f = 0.52$)²⁸ for the determination of the fluorescence quantum yield of the three triads incorporated into Triton X-100/BZN aqueous micelle solutions. All absorbances were matched at the excitation wavelength 590 nm. Emission was recorded in the range 600–800 nm.

Results

The absorption spectra for C–P–C₆₀, C–P–Q, and C–P–NQ in neat BZN and in freshly prepared Triton X-100 micelles are shown in Figure 1. A small blue shift is observed in the case of C–P–Q and C–P–NQ, and broader absorption bands in the case of C–P–C₆₀ when the triads are inside the micelles.

Fluorescence Data. No emission was found in the range 600–800 nm, indicating that the three triads dissolved in BZN and incorporated into Triton X-100 aqueous micelles do not fluoresce within our emission detection limit. This result is relevant for the calculation and analysis of the enthalpy content of the CS state $\text{C}^{\bullet+}\text{P}-\text{A}^{\bullet-}$ as discussed below.

LIOAS Data. The LIOAS signal obtained at 10 °C upon excitation at 650 nm of C–P–C₆₀, C–P–Q, and C–P–NQ dissolved in BZN within Triton X-100 aqueous micelles is shown in Figure 2, together with the signal of the calorimetric reference (azulene) taken under the same conditions, and the fits obtained in each case by convolution of the reference signal and the model function for the time evolution of the pressure

TABLE 1: Lifetimes τ_i and Pre-exponential Factors φ_i for the Production (1) and Decay (2 and 3) of the $C^{+}-P-A^{-}$ State Obtained from Deconvolution of the LIOAS Signals (All Degassed Samples) for the Three Triads C-P-C₆₀, C-P-Q, and C-P-NQ in Triton X-100/BZN Aqueous Micelles at Various Temperatures^a

sample	T/°C	τ_2 /ns	τ_3 /ns	φ_1	φ_2	φ_3
C-P-C ₆₀	20	47.6	776	0.536	0.244	0.087
	15	48.8	1500	0.486	0.283	0.107
	10	50.5	1200	0.507	0.235	0.136
	8	45.9	1500	0.427	0.304	0.148
	6	64.6	2160	0.502	0.256	0.120
	4	63.8	2190	0.357	0.333	0.184
C-P-Q	20	33.0	339	0.495	-0.046	0.362
	15	33.3	354	0.422	0.043	0.342
	10	32.1	386	0.374	0.108	0.335
	8	33.6	397	0.332	0.153	0.334
	6	30.7	361	0.286	0.174	0.344
	4	35.1	415	0.205	0.276	0.388
C-P-NQ	20	49.2	459	0.608	0.128	0.142
	15	47.6	487	0.569	0.143	0.162
	10	44.0	562	0.455	0.235	0.205
	8	45.4	612	0.419	0.238	0.215
	6	49.6	624	0.333	0.271	0.200
	4	53.2	669	0.162	0.336	0.366

^a In every case the value of τ_1 was <0.2 ns.

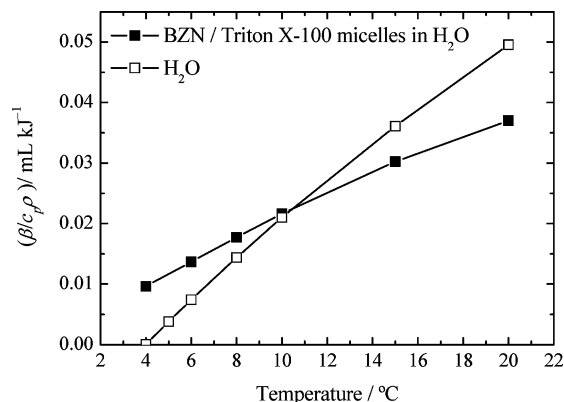


Figure 3. Ratio of thermoelastic parameters ($\beta/c_p\rho$) vs temperature for H₂O as obtained from tables and for the Triton X-100/BZN micelles in H₂O determined as described in the Experimental Section.

wave. Satisfactory fits of the LIOAS signals from the three samples were obtained using a three-exponential function. Six parameters were calculated from the fitting in each case, *i.e.*, three lifetimes (τ_1 , τ_2 , and τ_3) and three pre-exponential factors (φ_1 , φ_2 , and φ_3). By fixing τ_1 at any value between 0.1 and 1 ns, we obtained a similar value of the associated amplitude φ_1 . That means that these processes are faster than the time resolution of the experiment, and the amplitude φ_1 is a reliable measure of the amplitude of these processes.

The values of the lifetimes and the respective pre-exponential factors after excitation at 650 nm of C-P-C₆₀, C-P-Q, and C-P-NQ in Triton X-100/BZN aqueous micelles at various temperatures are collected in Table 1. The values of the ratio ($\beta/c_p\rho$)_{Tx} determined as described in the Experimental Section are plotted vs T in Figure 3.

The plots of φ_1 , φ_2 and φ_3 versus ($c_p\rho/\beta$)_{Tx} were linear for the three triads in the temperature range 4–20 °C, as predicted by eq 1. The results for C-P-C₆₀, C-P-Q, and C-P-NQ are shown in Figure 4.

LIOAS measurements were also performed with the triads in neat BZN. For this solvent, ($c_p\rho/\beta$)_{BZN} = 2.074 kJ mL⁻¹ is practically independent of temperature and much smaller than those for water or aqueous solutions. Two lifetimes and two

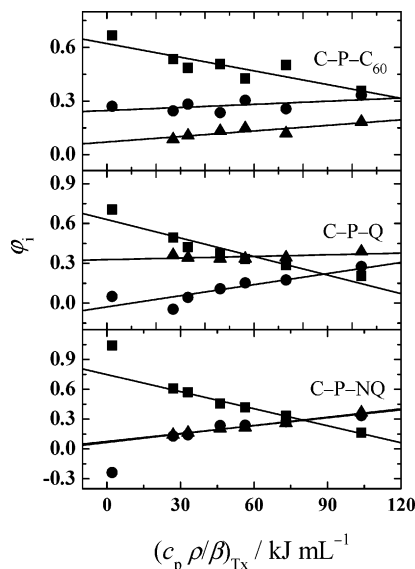


Figure 4. Amplitudes of the first (φ_1 , ■), second (φ_2 , ●) and third (φ_3 , ▲) exponential components of the pressure–time evolution, as derived from deconvolution of the LIOAS waveforms for C-P-C₆₀, C-P-Q, and C-P-NQ vs ($c_p\rho/\beta$)_{Tx} for the micelle medium. The values of the amplitudes corresponding to measurements with the respective triad in neat BZN are also included [($c_p\rho/\beta$) for BZN is 2.074 kJ/mL].

pre-exponential factors were necessary to fit the LIOAS signals of the triads dissolved in neat BZN. The values of the LIOAS amplitudes obtained in neat BZN fall satisfactorily, especially for C-P-C₆₀ and C-P-Q, within the linear correlation regime found for the micellar media (see Figure 4).

Transient Absorbance Data: Quantum Yields of Charge Separation in Micelles. The $C^{+}-P-A^{-}$ state shows a strong transient absorption in the 950–1000 nm region assigned to the carotenoid radical cation (centered at *ca.* 980 nm).¹⁹ The decay of the transient absorption at 960 nm [$\Delta A(960)$] after excitation of the three triads at 650 nm in Triton X-100/BZN aqueous micelles (Figure 5) was fitted in every case with a biexponential model:

$$\Delta A(960) = A_1 \exp(-t/\tau_{A_1}) + A_2 \exp(-t/\tau_{A_2}) \quad (4)$$

The shorter decay time τ_{A_1} (48 ± 2 , 49 ± 6 , and 32 ± 3 ns for $C^{+}-P-C_{60}^{-}$, $C^{+}-P-NQ^{-}$, and $C^{+}-P-Q^{-}$, respectively) was very similar to the lifetime τ_2 found in the LIOAS experiments (see Table 1). A longer-lived component, with small amplitude for C-P-C₆₀ and C-P-Q and a decay time between 400 and 1200 ns (depending on the triad) was required to fit the transient absorption data. This longer lifetime agrees in general with the lifetime τ_3 found in the LIOAS experiments and may correspond to the decay of $C^{+}-P-A^{-}$ in a less polar environment. When comparing the decay times of the $C^{+}-P-A^{-}$ state in micelles and in neat BZN (66 ± 1 ns, 30 ± 1 ns, and 57 ± 1 ns for $C^{+}-P-C_{60}^{-}$, $C^{+}-P-NQ^{-}$, and $C^{+}-P-Q^{-}$, respectively), we observed some differences in the lifetimes of the $C^{+}-P-A^{-}$ state. The different environment of the supermolecules in both cases may be the reason for these observations.

The quantum yields for the formation of $C^{+}-P-A^{-}$, Φ_{CS} , for the three triads in Triton X-100/BZN aqueous micelles are required to calculate the changes in the thermodynamic parameters upon formation of $C^{+}-P-A^{-}$. They were determined by comparing the transient absorbance extrapolated to zero time of the carotenoid radical cation at 960 nm after excitation of

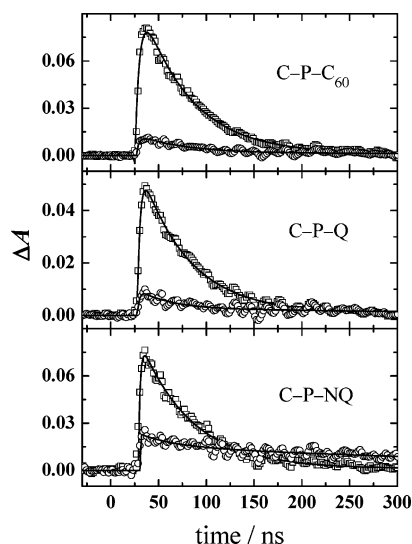


Figure 5. Transient absorption decay kinetics at 960 nm for the three triads in Triton X-100/BZN aqueous micelle solutions (O) following excitation at 650 nm with a 5 ns laser pulse. C-P-C₆₀ in deoxygenated 2-methyltetrahydrofuran was used as reference (□) for the three triads. A two-exponential fit of the data (see text) is shown as a full curve line. The absorbances of the solutions at 650 nm were *ca.* 0.014, 0.050, and 0.094 for C-P-C₆₀, C-P-NQ and C-P-Q, respectively (laser energy *ca.* 2 mJ/pulse). The measurements were all performed at room temperature in the linear regime of amplitude versus laser radiant energy.

the triad with that of a matched absorbance solution of C-P-C₆₀ dissolved in 2Me-THF. The quantum yield of C^{•+}-P-C₆₀^{•-} formation in 2Me-THF was previously found to be 1.0.¹⁹ The sum of the pre-exponential factors of the biexponential fitting function ($A_1 + A_2$, eq 4) was used for this determination. A correction for the difference in the refractive indices of the solvents (eq 5) was applied for the calculation of the quantum yield Φ_{CS} , in view of the fact that the reference and the samples were not dissolved in the same solvent²⁹

$$\Phi_{cs}^S = \frac{\Delta A_S n_S^2}{\Delta A_R n_R^2} \Phi_{cs}^R \quad (5)$$

In eq 5, ΔA is the transient absorption change at zero time ($A_1 + A_2$, eq 4) S and R superscripts and subscripts refer to sample and reference, respectively, and n is the respective refractive index of the solvent containing the reference (2 Me-THF, $n = 1.4059$) and the sample (BZN/Triton X-100/water mixture, $n = 1.3420$). The yields determined in this way were $\Phi_{CS} = 0.11 \pm 0.01$, 0.25 ± 0.03 , and 0.15 ± 0.01 for the formation of C^{•+}-P-C₆₀^{•-}, C^{•+}-P-NQ^{•-}, and C^{•+}-P-Q^{•-}, respectively, in Triton X-100/BZN aqueous micelles. With the values of A_1 and A_2 (eq 4), and assuming the same absorption coefficient for the CS state in the different media and environment, the separate quantum yields for the CS short-lived (Φ_2) and long-lived (Φ_3) decays, respectively, were calculated as $\Phi_2 = 0.106$ and $\Phi_3 = 0.01$ for C-P-C₆₀, $\Phi_2 = 0.09$ and $\Phi_3 = 0.18$ for C-P-NQ, and $\Phi_2 = 0.11$ and $\Phi_3 = 0.04$ for C-P-Q.

TR-EPR Data. Because of the high dielectric constant of water, TR-EPR measurements were not possible with micelle solutions at room temperature. Although aware of the fact that the low-temperature processes might differ from those at room temperature, TR-EPR measurements at 40 K were performed to detect the presence of the carotene triplet state by charge recombination of the CS state. The signals obtained with C-P-C₆₀ in 2-Me-THF and in BZN (Figure 6) demonstrate that in

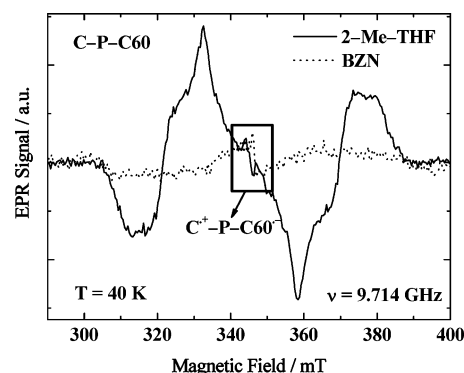
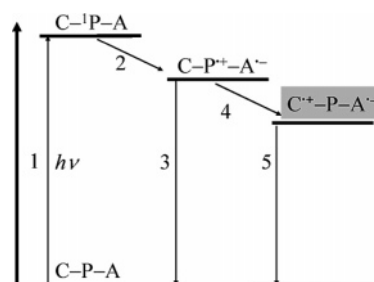


Figure 6. TR-EPR spectra of triad C-P-C₆₀ in 2-Me-THF and in BZN. The spectrum is dominated by the contribution of the carotene triplet state.³⁰ A low-intense CS biradical signal is present in the center of the spectrum.

SCHEME 2: Term Diagram of the Photoinitiated Processes in C-P-A^a



^a The energy levels of the various species are not located at scale.

the former solvent the carotene triplet is formed, whereas in the latter no triplet carotene is observed. In both cases, however, a narrow signal is observed at 3440 G, attributable to the CS radical pair state, C^{•+}-P-C₆₀^{•-}.³⁰ No TR-EPR signal was detected when the experiment was performed in Triton X-100 micelles at 40 K, due to the strongly reduced concentration of supermolecules in the micellar solution as compared to the neat solvents.

Discussion

Several consecutive processes occur upon excitation of the C-P-A “supermolecules” within the porphyrin Q-absorption band at 650 nm.

Excitation of P is followed by photoinduced ET to the acceptor to yield C-P^{•+}-A^{•-}. Rapid ET from the carotene to the porphyrin radical cation yields the CS state with $\Phi(C^{\bullet+}-P-C_{60}^{\bullet-}) = 0.11$, $\Phi(C^{\bullet+}-P-Q^{\bullet-}) = 0.15$, and $\Phi(C^{\bullet+}-P-NQ^{\bullet-}) = 0.25$ for the triads incorporated within Triton X-100/BZN aqueous micelle solutions (see Scheme 2).

The value of Φ_{CS} when C₆₀ is the acceptor is much lower than that measured in neat BZN ($\Phi_{CS} = 0.80$). There may be several reasons for this effect. An important consideration is that the C-P-C₆₀ triads may localize with the carotene in the detergent region and the fullerene in BZN, in addition to conformational changes of the “supermolecule” or aggregation phenomena. Aggregation could induce radiationless fluorescence quenching in competition with charge separation whereas conformational changes could induce a more rapid electron back transfer than that observed in homogeneous solution. In principle, energy transfer from porphyrin to C₆₀ could be discounted, because no C₆₀ triplet was observed during the flash photolysis experiments with optical detection. Should porphyrin-C₆₀ energy transfer be operative, triplet C₆₀ would be

TABLE 2: Quantum Yields, Φ_{CS} , for the Formation; Structural Volume Changes, $\Delta_{str,i}V$ for the Formation and $\Delta_{str,2}V$ and $\Delta_{str,3}V$ for the Decay, of the C^{*+} -P-A $^{-}$ State for the Three Triads; and $\Delta_{CS}H^0$, $\Delta_{CS}G^0$ and $T\Delta_{CS}S^0$ for the CS State Formation from the Respective Ground State Triad

	C-P-C ₆₀	C-P-NQ	C-P-Q
Φ_{CS}	0.11	0.25	0.15
$\Delta_{str,1}V/(\text{mL mol}^{-1})^{a,b}$	-4.2	-4.2	-5.7
$\Delta_{str,2}V/(\text{mL mol}^{-1})^{a,b}$	1.5	5.7	4.7
$\Delta_{str,3}V/(\text{mL mol}^{-1})^{a,b}$	c	1.1	1.9
$\Delta_{CS}H^0/(\text{kJ mol}^{-1})^{a,b}$	633	184	454
$\Delta_{CS}G^0/(\text{kJ mol}^{-1})$	141	143	125
$\Delta_{ET}G^0/(\text{kJ mol}^{-1})^d$	-43	-41	-59
$T\Delta_{CS}S^0/(\text{kJ mol}^{-1})$	492	41	329

^a ΔV and ΔH are per mole of CS state formed. ^b Errors are <10% for Φ and ΔV and $\pm 40\%$ for q , and consequently, also $\pm 40\%$ for ΔH^0 .

^c The very low quantum yield of this process, Φ_3 , affords a value with a very large error. ^d For the ET from the excited state, *i.e.*, considering the excitation energy.

observed at 700 nm. An alternative explanation could be that, in view of the formation of two types of micelles (spherical and ellipsoidal) in 0.1 M Triton in the presence of organic solvents (BZN in our case),³¹ only one of the hosts would permit ET, whereas in the other one radiationless deactivation without ET could occur. These different localizations of the dyads, also depending on the size of the dyad, may explain the different lifetimes observed in homogeneous medium *vs* those in the micelles. These possibilities have not been analyzed further.

In contrast, the values of Φ_{CS} when the planar quinones are the acceptors are similar to those obtained in neat BZN.^{19,21} The formation of C^{*+} -P-A $^{-}$ occurs in *ca.* 150 ps for the three triads.¹⁶ The long-lived CS state decays to the ground state.¹⁶ No evidence of carotene triplet formation was found with any of the triads dissolved in neat BZN by low-temperature TR-EPR measurements upon 650 nm excitation, indicating that recombination to give some carotene triplet is not operative at low temperature in polar solvents (Figure 6). Flash photolysis experiments performed at room temperature with the triads dissolved in Triton X-100/BZN aqueous micelles, monitoring the transient absorption at 540 nm (where the carotene triplet state absorbs), confirm this result for C-P-Q and C-P-NQ. In the case of C-P-C₆₀ within Triton X-100/BZN aqueous micelles, recombination yields some carotene triplet states (<10%) as observed by transient absorption experiments at room temperature.

The LIOAS amplitude φ_1 is a measure of the C^{*+} -P-A $^{-}$ production, taking into account that this state is formed in some hundreds of ps. The second and third amplitudes, φ_2 and φ_3 , and their respective decay times, correspond to the C^{*+} -P-A $^{-}$ decay (most probably in two different environments within the micelles).

The intercept q_1/E_λ of the linear plots of φ_1 *vs* $(c_p\rho/\beta)_{TX}$ (Figure 4) yields q_1 , *i.e.*, the heat released during C^{*+} -P-A $^{-}$ formation. Taking into account that the steady state fluorescence experiments with the triads in Triton X-100/BZN aqueous micelles showed that none of the triads fluoresce, simple energy balance considerations afford the enthalpy content $\Delta_{CS}H$ through

$$E_\lambda = q_1 + \Delta_{CS}H \Phi_{CS} \quad (6)$$

The values of $\Delta_{CS}H$ are positive (Table 2); *i.e.*, the formation of the long-lived CS state from the ground state is endothermic. For C-P-C₆₀ and C-P-Q, $\Delta_{CS}H$ is larger than that for C-P-NQ. The $\Delta_{CS}H$ for C-P-NQ is similar to the molar energy of the laser pulse. It is important to realize that although the intercepts of the lines of φ_1 *vs* $(c_p\rho/\beta)_{TX}$ in Figure 4 are all

similar within the experimental error, the different quantum yields for the formation of the CS states in the three “super-molecules” give rise to different values for the enthalpy content of the CS species in each case. The low quantum yields and the errors associated with their determination for C-P-C₆₀ and C-P-Q make any speculation about the differences in these values difficult. However, even if the $\Delta_{CS}H$ values for C-P-C₆₀ and C-P-Q are similar within the large experimental error, they are definitively larger than $\Delta_{CS}H$ for C-P-NQ.

The standard Gibbs energy, $\Delta_{ET}G^0$, for the formation of the CS state from the excited state was calculated using

$$\Delta_{ET}G^0 = N_A \{ e[E^0(D^{*+}/D) - E^0(A/A^{*+})] + w_{D^{*+}A^{*+}} - w_{DA} \} - E_\lambda \quad (7)$$

with $w_{DA} = z_D z_A e^2 / (4\pi\epsilon_0 \epsilon_r a) = 0$ in our case and $w_{D^{*+}A^{*+}} = [N_A(u^2)/(4\pi\epsilon_0 \rho^3)] [(\epsilon_r - 1)/(2\epsilon_r + 1)]$.

In the above equation, a is the distance between donor and acceptor before ET, ϵ_r is the relative medium static permittivity, ϵ_0 is the electric constant (formerly called vacuum permittivity), and z_X the charge of the species X. The equation given above considers a linked donor and acceptor for the calculation of $w_{D^{*+}A^{*+}}$, *i.e.*, the stabilization or destabilization of a dipole moment μ in a cavity of radius ρ .³²

In the case of a similar C-P-C₆₀ “supermolecule”, a very large dipole moment $\mu = 150$ D was evaluated upon charge separation under the assumption of a linear configuration of the molecule and a distance of *ca.* 32 Å between the charged centers.¹ With these values, $w_{D^{*+}A^{*+}} = 19$ kJ mol⁻¹ is calculated in BZN with the above expression.

A more folded conformation arising from the so-called harpooning mechanism,^{33,34,36} leads to smaller values of the dipole moment but larger values of $w_{D^{*+}A^{*+}}$ due to the smaller radius ρ of the cavity. In fact, Smirnov *et al.*¹ indicate that formation of the radical cation may lead to a collapsed more closed conformation in which the center of the negatively charged acceptor unit would be nearer the center of the carotene backbone. Preliminary semiempirical gas-phase calculations (UHF/3-21G), with tetracyano quinone instead of naphthoquinone, also favor such conformations for the CS state.³⁷ In this case, the dipole moment would be *ca.* 110 D.¹ We note that similar calculations with other “supermolecules” afforded values for the intercharge distance and other molecular parameters fully confirmed by experimental data.^{35,38,39}

With the value of 110 D for the dipole moment and a distance between the center of gravity of the opposite charges of about 20 Å, a value $w_{D^{*+}A^{*+}} = 42$ kJ mol⁻¹ is calculated in BZN with the above expression. In other words, the CS state is destabilized by 42 kJ mol⁻¹ due to the harpooning mechanism. This value can also be used for the C-P-Q and C-P-NQ “supermolecules” as the possible Coulombic contribution to the Gibbs energy for the production of the charge separated state. Thus, $w_{D^{*+}A^{*+}} = 42$ kJ mol⁻¹ was used in all three cases for the calculation of the $\Delta_{CS}G^0$ values listed in Table 2. This is a very large value, and therefore, the $\Delta_{CS}G^0$ values should be considered as upper limits.

The standard potentials used for the calculations of the $\Delta_{CS}G^0$ values (see Table 2) for the donor were $E^0(D^{*+}/D) = E^0(C^{*+}/C) = 0.47$ V *vs* SCE (for the carotenoid of C-P-C₆₀ and C-P-NQ),¹⁹ and 0.55 V (for the carotenoid of C-P-Q);⁴⁰ for the three acceptors they were $E^0(A/A^{*+}) = E^0(C_{60}/C_{60}^{*+}) = -0.56$ V,¹⁹ $E^0(Q/Q^{*+}) = -0.31$ V,⁴¹ and $E^0(NQ/NQ^{*+}) = -0.58$ V *vs* SCE.⁴²

The values of $\Delta_{CS}G^0$ in Table 2 are for the process from the respective ground state triad, *i.e.*, without the excitation energy (contrary to the values of $\Delta_{ET}G^0$ which include E_λ and are, therefore, <0). Application of the Gibbs energy relationship together with the data for $\Delta_{CS}H^0$ affords the values of the entropic term for the CS state formation from the ground state in each case (Table 2).

The entropic term is dominant at room temperature in Triton X-100/BZN aqueous micelles for C-P-C₆₀ and for C-P-Q. It is, however, not so large, though relatively important, for C-P-NQ. The enthalpy content for C-P-C₆₀ and C-P-Q is 633 and 454 kJ mol⁻¹, respectively. In these two cases the high entropic term during the charge separation at room temperature should be attributed to the reorganization of the solvent molecules induced by the very large photoinduced dipole moment.

The sum of the intercepts q_2/E_λ and q_3/E_λ of the linear plots using φ_2 and φ_3 (Figure 4) yields the total heat released during the decay of the C^{•+}-P-A^{•-} (both long- and short-lived states). The values of $(q_2 + q_3)/\Phi_{CS}$ are *ca.* 458, 252, and 0 kJ mol⁻¹ for C-P-C₆₀, C-P-NQ, and C-P-Q, respectively. The heat released in the case of C-P-NQ is similar to $\Delta_{CS}H$, within the large error of the determinations, indicating that the CS state goes back to the ground state with a quantum yield of 100%. In the case of C-P-C₆₀ and C-P-Q, the heat released is lower than $\Delta_{CS}H$, particularly for C-P-Q. We take this as an indication that other species are in part produced upon CS decay and store part of the energy. This is supported by the fact that the solutions of all compounds, but more rapidly of C-P-C₆₀, suffer permanent bleaching after a large number of laser pulses, or upon standing in the light for some hours. We have used for these calculations the total decay quantum yield, to compare the total heat released with the heat of formation, calculated using the Gibbs equation (see Table 2).

We have already indicated that in BZN there is no formation of carotene triplet states upon charge recombination of the CS states in the triads containing quinones as electron acceptors. Therefore, these energy storing long-lived species are most likely related to the decomposition products of the samples. In the case of C-P-C₆₀, the species storing some energy may be related to the formation of some carotene triplet state, as seen in our flash photolysis experiments in Triton X-100/BZN aqueous micelles performed at room temperature.

The slopes of the plots of φ_1 vs $(c_p/\beta)_{Tx}$ yield the structural volume changes per absorbed einstein involved in the formation of the respective C^{•+}-P-A^{•-} state. The molar values of the structural volume changes, $\Delta_{str,1}V$, *i.e.*, the slopes of the plots in Figure 4 divided by the quantum yield for the formation of the CS state, and multiplied by the laser pulse molar energy (eq 1), are listed in Table 2. For the three supermolecules, $\Delta_{str,1}V$ is negative; *i.e.*, a contraction is concomitant with the formation of the C^{•+}-P-A^{•-} state. $\Delta_{str,1}V$ is larger for C-P-Q, the triad containing a carboxylate group attached to the quinone, indicating that probably there is a stronger interaction of the carboxylate with the polar benzonitrile.

The Drude-Nernst equation for electrostriction, which describes the contraction taking place in a dielectric medium upon introduction of an ion, could be used for the calculation of the volume change induced in the BZN medium when the C^{•+}-P-A^{•-} state is formed. Because in our case a large dipole is created upon PET, eq 8, derived for the dipolar case, was used,⁴³ where $\Delta_{el}V$ represents the electrostriction volume change, μ is the dipole moment of the solute, r is the effective cavity

$$\Delta_{el}V = -\left(\frac{\mu^2}{r^3}\right) \frac{(\epsilon_r + 2)(\epsilon_r - 1)}{(2\epsilon_r + 1)^2} \kappa_T \quad (8)$$

radius, ϵ_r is the solvent dielectric constant and κ_T is the isothermal compressibility of the solvent.

Considering the value of 110 D for the dipole moment, a distance between the center of gravity of the opposite charges of 20 Å, $\epsilon_r = 25$ for BZN and $\kappa_T = 6.5 \times 10^{-10}$ Pa⁻¹, a contraction of *ca.* -14.5 mL mol⁻¹ is calculated. This volume contraction would be observed if only electrostriction (arising from the attraction of the polar solvent molecules toward the charged centers of the dipole) would be the cause of the volume change. The fact that we observe a lower contraction for the formation of the CS state than predicted indicates that a simultaneous expansion is occurring. Taking into account the calculated possible shape of the CS state (albeit the calculation implies several approximations), *i.e.*, that the charge separation may approach the positively charged acceptor end toward the center of the negatively charged carotene backbone (a harpoon-ing mechanism), some extrusion of solvent from the inner molecular cavity may produce simultaneously an expansion, thus reducing the value of the expected volume contraction.

The structural volume changes produced upon decay of the CS states may be calculated from the slopes of the φ_2 and φ_3 plots (Figure 4, Table 2). Using the corresponding values of Φ_2 and Φ_3 (see Results), the values of $\Delta_{str,2}V$ and $\Delta_{str,3}V$ listed in Table 2 are obtained. They are all expansions, as expected, in contrast to the contraction observed upon CS state formation. $\Delta_{str,3}V$ for C-P-C₆₀ could not be calculated due to the large error of Φ_3 .

We tried to evaluate the Marcus reorganization energy (λ) for the different triads into the micelles by performing nanosecond experiments as a function of temperature. The short range of temperature that could be used (277–293 K; lower temperatures were not possible because the micelle solutions freeze below 277 K) impaired the study of the temperature dependence of the CS decay rate constant. Therefore, the evaluation of the Marcus reorganization energy (λ) and its possible correlation with $\Delta_{str}V$ was not feasible. In any case, our results show that the measured contractions, although similar, are larger for C-P-Q than for C-P-C₆₀ and C-P-NQ.

Conclusions

Using micelles composed of benzonitrile and the “supermolecules” suspended in aqueous solution, and thus establishing a micellar nanoreactor, it was possible to separate the enthalpy and structural volume change contributions to the LIOAS signals upon photoinduced formation of the long-lived CS state C^{•+}-P-A^{•-}. The quantum yields for the formation of C^{•+}-P-A^{•-} for the three triads in Triton X-100/BZN aqueous micelles were evaluated by nanosecond-transient absorption. The volume contractions observed upon production of C^{•+}-P-A^{•-} for A = C₆₀, Q, and NQ are attributed to the solvent movements from the immediate environment of the molecule upon formation of the giant dipole. These contractions are similar for the three triads and found to be the largest for C-P-Q. There are remarkable differences in the enthalpy and entropy changes for the three different acceptors. Entropy changes attributed to solvent movements control the process of ET. The entropy changes for C-P-C₆₀ and C-P-Q are found to be larger than for C-P-NQ. The difference could be a consequence of the different Marcus reorganization energies determined for the different acceptors, especially considering the polar carboxylate group present in C-P-Q.

The heat released during the decay of one mole of charge separated state in the case of C–P–C₆₀ and C–P–Q, is smaller than its enthalpy content calculated as $\Delta H = (E_\lambda - q_1)/\Phi_{CS}$. This is attributed to the formation of long-lived energy storing species upon CS decay, especially in the case of C–P–Q, probably due to intermediates related to the decomposition of the “supermolecules”. In the case of C–P–C₆₀, the species storing some energy may be related to the formation of some carotene triplet state.

The method described in this work of including the supermolecular triads dissolved in BZN in Triton X-100 micelle nanoreactors is of great importance because it permits the measurements of the thermodynamic parameters for the formation of relatively short-lived species in polar nonaqueous media of isolated molecules included in micelles. We have used the enthalpy change determined by LIOAS together with the free energy for the photoinduced reaction to calculate the intrinsic entropy of the reaction. The entropic terms obtained are very large, indicating that entropy cannot be neglected in ET reactions.

Acknowledgment. We are grateful to Professor Wolfgang Lubitz (MPI-BAC) for his continuous support and for providing the equipment for the EPR measurements A.C.R. and S.E.B. gratefully thank Aba Losi (Università degli Studi di Parma) and Elsa Abuin (Universidad de Santiago de Chile) for valuable suggestions, Michael Paddon-Row (University of New South Wales, Sydney) for preliminary calculations of the CS state conformation, and Toby D. M. Bell (Melbourne) for preliminary experiments. The technical help by Dagmar Lenk, Gül Koc, and Simone Möllenbeck is also gratefully acknowledged. This work was generously supported by the Volkswagen Foundation (Az:I/77 588) within the Program on “Electron Transfer” and by the US Department of Energy (FG02-03ER15393).

References and Notes

- (1) Smirnov, S. N.; Liddell, P. A.; Vlassioun, I. V.; Teslja, A.; Kuciauskas, D.; Braun, C. L.; Moore, A. L.; Moore, T. A.; Gust, D. *J. Phys. Chem. A* **2003**, *107*, 7567–7573.
- (2) Steinberg-Yfrach, G.; Rigaud, J. L.; Durantini, E. N.; Moore, A. L.; Gust, D.; Moore, T. A. *Nature* **1998**, *392*, 479–482.
- (3) Kuciauskas, D.; Liddell, P. A.; Lin, S.; Stone, S. G.; Moore, A. L.; Moore, T. A.; Gust, D. *J. Phys. Chem. B* **2000**, *104*, 4307–4321.
- (4) Imahori, H.; Mori, Y.; Matano, Y. *J. Photochem. Photobiol. C: Photochem. Rev.* **2003**, *4*, 51–83.
- (5) Marcus, R. A.; Sutin, N. *Biochim. Biophys. Acta* **1985**, *811*, 265–322.
- (6) Marcus, R. A. *Angew. Chem., Int. Ed. Engl.* **1993**, *32*, 1111–1121.
- (7) Bixon, M.; Jortner, J. *Adv. Chem. Phys.* **1999**, *106*, 35–202.
- (8) Peters, K. S.; Snyder, G. J. *Science* **1988**, *241*, 1053–1057.
- (9) Braslavsky, S. E.; Heibel, G. E. *Chem. Rev.* **1992**, *92*, 1381–1410.
- (10) Gensch, T.; Viappiani, C.; Braslavsky, S. E. In *Encyclopedia of Spectroscopy and Spectrometry*; Lindon, J. L., Tranter, G. E., Holmes, J. L., Eds.; Academic Press: New York, 1999; pp 1124–1132.
- (11) Losi, A.; Braslavsky, S. E. *Phys. Chem. Chem. Phys.* **2003**, *5*, 2739–2750.
- (12) Gensch, T.; Viappiani, C. *Photochem. Photobiol. Sci.* **2003**, *2*, 699–721.
- (13) Rudzki, J. E.; Goodman, J. L.; Peters, K. S. *J. Am. Chem. Soc.* **1985**, *107*, 7849–7854.
- (14) Borsarelli, C. D.; Braslavsky, S. E. *J. Phys. Chem. B* **1998**, *102*, 6231–6238.
- (15) Borsarelli, C. D.; Braslavsky, S. E. *J. Phys. Chem. A* **1999**, *103*, 1719–1727.
- (16) Moore, T. A.; Moore, A. L.; Gust, D. *Philos. Trans. R. Soc. London B* **2000**, *357*, 1481–1498.
- (17) Carbonera, D.; Di Valentin, M.; Corvaja, C.; Agostini, G.; Giacometti, G.; Liddell, P. A.; Kuciauskas, D.; Moore, A. L.; Moore, T. A.; Gust, D. *J. Am. Chem. Soc.* **1998**, *120*, 4398–4405.
- (18) Martínez-Junza, V.; Rizzi, A.; Jolliffe, K. A.; Head, N. J.; Paddon-Row, M. N.; Braslavsky, S. E. *Phys. Chem. Chem. Phys.* **2005**, *7*, 4114–4125.
- (19) Kodis, G.; Liddell, P. A.; Moore, A. L.; Moore, T. A.; Gust, D. *J. Phys. Org. Chem.* **2004**, *17*, 724–734.
- (20) Hung, S.-C. Dissertation, Arizona State University, 1995.
- (21) Steinberg-Yfrach, G.; Liddell, P. A.; Hung, S.-C.; Moore, A. L.; Moore, T. A.; Gust, D. *Nature* **1997**, *385*, 239–241.
- (22) C–P–NQ was prepared by the same procedure described in ref 19 for a similar triad.
- (23) Eastoe, J.; Crooks, E. R.; Beeby, A.; Heenan, R. K. *Chem. Phys. Lett.* **1995**, *245*, 571–577.
- (24) Gensch, T.; Viappiani, C.; Braslavsky, S. E. *J. Am. Chem. Soc.* **1999**, *121*, 10573–10582 and references therein.
- (25) Borsarelli, C. D.; Braslavsky, S. E. *J. Phys. Chem. B* **1997**, *101*, 6036–6042.
- (26) Srivastava, A. P. *Indian J. Chem.* **1992**, *31 A*, 577–580.
- (27) Davis, F. S.; Nemeth, G. A.; Anjo, D. M.; Makings, L. R.; Gust, D.; Moore, T. A. *Rev. Sci. Instrum.* **1987**, *58*, 1629–1631.
- (28) Magde, D.; Brannon, J. H.; Cremers, T. L.; Olmsted, J. *J. Phys. Chem.* **1979**, *83*, 696–699.
- (29) Eaton, D. F. *Pure Appl. Chem.* **1988**, *60*, 1107–1114.
- (30) Di Valentin, M.; Bisol, A.; Giacometti, G.; Carbonera, D.; Agostini, G.; Liddell, P.; Moore, A. L.; Moore, T. A.; Gust, D. *Mol. Cryst. Liq. Cryst.* **2003**, *394*, 19–30.
- (31) Mishael, Y. G.; Dubin, P. L. *Langmuir* **2005**, *21*, 9803–9808.
- (32) Böttcher, C. J. F. *Theory of Electrical Polarization*; Elsevier: Amsterdam, 1973; p 145.
- (33) Wegewijs, B.; Hermant, R. M.; Verhoeven, J. W.; de Haas, M. P.; Warman, J. M. *Chem. Phys. Lett.* **1987**, *140*, 587–590.
- (34) Lauteslager, X. Y.; van Stokkum, I. H. M.; van Ramesdonk, H. J.; Brouwer, A. M.; Verhoeven, J. W. *J. Phys. Chem. A* **1999**, *103*, 653–659.
- (35) Wegewijs, B.; Verhoeven, J. W. *Adv. Chem. Phys.* **1999**, *106*, 221–264.
- (36) Shephard, M. J.; Paddon-Row, M. N. *J. Phys. Chem. A* **2000**, *104*, 11628–11635.
- (37) Preliminary calculations carried out by M. J. Shephard and M. N. Paddon-Row (Sydney, Australia).
- (38) Shephard, M. J.; Paddon-Row, M. N. *J. Phys. Chem. A* **1999**, *103*, 3347–3350.
- (39) Bell, T. D. M.; Jolliffe, K. A.; Ghiggino, K. P.; Oliver, A. M.; Shephard, M. J.; Paddon-Row, M. N. *J. Am. Chem. Soc.* **2000**, *122*, 10661–10666.
- (40) Sereno, L.; Silber, J. J.; Otero, L.; Bohorquez, M. del V.; Moore, A. L.; Moore, T. A.; Gust, D. *J. Phys. Chem.* **1996**, *100*, 814–821.
- (41) Hung, S.-C.; Macpherson, A. N.; Lin, S.; Liddell, P. A.; Seely, G. R.; Moore, A. L.; Moore, T. A.; Gust, D. *J. Am. Chem. Soc.* **1995**, *117*, 1657–1658.
- (42) Kuciauskas, D.; Liddell, P. A.; Hung, S. C.; Lin, S.; Stone, S.; Seely, G. R.; Moore, A. L.; Moore, T. A.; Gust, D. *J. Phys. Chem. B* **1997**, *101*, 429–440.
- (43) Wegewijs, B.; Paddon-Row, M. N.; Braslavsky, S. E. *J. Phys. Chem. A* **1998**, *102*, 8812–8818.